JOURNAL OF PROPULSION AND POWER
Vol. 23, No. 1, January–February 2007

Computational Study of Primary Electron Confinement by Magnetic Fields in the Discharge Chamber of an Ion Engine

Sudhakar Mahalingam* and James A. Menart†
Wright State University, Dayton, Ohio 45435

DOI: 10.2514/1.18366

A computational investigation of the ability of different magnetic field shapes to confine primary electrons in a discharge chamber of an ion engine is performed. Ideal and actual magnetic fields are studied to gain an understanding of which magnetic field shape provides the most primary electron confinement. The simple, ideal field studies clearly show that particle collisions significantly reduce the confinement ability of a magnetic field. The design parameter studied for actual ring-cusp configurations is the number of magnetic rings used on the discharge chamber. This study indicates that adding additional magnet rings to the discharge chamber does not necessarily increase the confinement ability of the magnetic field. For the size discharge chamber studied in this work, increasing the number of magnetic rings reduces the confinement ability of the magnetic field.

I. Introduction

ONE important design consideration for the discharge chamber of an ion engine is how well the magnetic field confines primary electrons. This work is a computational investigation of the ability of different magnetic field shapes to confine primary electrons in the discharge chamber of an ion engine. Ideal and actual magnetic fields are studied to gain an understanding of which magnetic field shape provides the best primary electron confinement. Simple, ideal field studies are used to investigate the magnitude of magnetic fields required to confine primary electrons when the field lines are parallel to the wall being shielded, to study the effects of holes in the magnetic field, and to study the effect of particle collisions. The magnetic field design parameter studied for actual ring-cusp configurations is the number of magnetic rings used on the discharge chamber. This study indicates that adding additional magnet rings to the discharge chamber does not increase the confinement ability of the magnetic field.

Computer modeling can be an effective tool in analyzing the primary electron confinement ability of a magnetic field. If this type of work is done experimentally the cost quickly becomes prohibitive. Computer modeling allows one to perform parametric studies quickly and inexpensively. In this work, a computer code called PRIMA [1] is used for this purpose. PRIMA is a numerical model that tracks primary electrons throughout the discharge chamber of an ion engine accounting for the effects of magnetic fields and collisions. The version of PRIMA used in this work is one that has been updated from a version produced by Arakawa and Yamada [2]. The primary capability of PRIMA is determining how well primary electrons are contained in the discharge chamber by the magnetic field.

Some investigators who have studied the effects of magnet fields are Isaacson and Kaufman [3], Kaufman et al. [4], Ramsey [5], Sovey [6], Brophy and Wilbur [7], Matossian and Beattie [8], Beattie and Matossian [9], Sandonato et al. [10], and Wirz and Katz [11]. Most of these investigations perform comparisons between different types of magnetic fields such as divergent fields, multicusp fields, line-cusp fields, and ring-cusp fields. Some looked at variations in the multicusp field. Except for Sovey [6] and Beattie and Matossian [9], no investigation into an optimum ring-cusp magnetic field was made. Sovey [6] considered 15 ring-cusp variants and Beattie and Matossian [9] appear to have looked at three configurations. This is not a great deal of ring-cusp configurations to study. Because both of these investigations are experimental it has to be costly to look at many different configurations. In this work, the confinement merits of different ring-cusp magnetic fields are studied from a computational perspective. Whereas there is still a great deal of work involved in this type of study from a computational perspective, it is much less expensive than an experimental perspective. This paper shows a sample of the ring-cusp magnetic field configurations that were studied computationally by the authors. More results can be found in [1]. Of the investigations listed, Sandonato et al. [10] and Wirz and Katz [11] are the only ones to study magnetic field configurations from a computational perspective. Sandonato et al. [10] studied a multicusp, a line-cusp, and a ring-cusp configuration, but did not optimize the ring-cusp configuration. Wirz and Katz [11] did some interesting work looking at the effect of increasing the strength of the middle magnetic ring on an NSTAR thruster.

II. Computational Model Description

In this work, two computational tools, PANDIRA and PRIMA, are being used to model the magnetic field and the primary electron trajectories in the discharge chamber of an ion engine. PANDIRA [12] is a magnetic field solver that determines the magnetic fields in the discharge chamber exactly by solving Maxwell's equations. PRIMA solves the equations of motion for primary electrons in an axisymmetric discharge chamber to determine their trajectory. Information on the implementation of PANDIRA for magnetic field modeling in a discharge chamber and details on PRIMA can be found in the work of Mahalingam and Menart [1].

The most important output quantities from PRIMA are the average primary electron confinement length and the relative primary electron number densities. The average primary electron confinement length is the average distance traveled by a primary electron during its lifetime in the discharge chamber. The larger the confinement length, the better the magnetic field confines the primary electrons. The confinement length in nondimensional form is the deciding parameter for the comparisons presented in this work. A nondimensional confinement length is a dimensional confinement length that has been divided by the discharge chamber diameter. The

Received 24 June 2005; revision received 7 April 2006; accepted for publication 10 April 2006.

*Ph.D. Candidate, Mechanical and Materials Engineering Department, 209 RC. Student Member AIAA.

†Associate Professor, Mechanical and Materials Engineering Department, 123 RC. Member AIAA.

other primary result obtained from PRIMA is the relative primary electron number density. The relative primary electron number density is the ratio of the actual primary electron number density at a given location in the discharge chamber to the maximum primary electron number density observed in the discharge chamber.

Comparisons of results from PRIMA to the experimental results of Hiatt and Wilbur [13] can be found in Deshpande et al. [14] The comparisons reported in this source are within 18%. This indicates that PRIMA is predicting reasonable values for confinement lengths and is therefore an acceptable tool to use in a magnetic field confinement study.

III. Simple, Ideal Magnetic Field Results

In addition to being less costly to perform than experimental investigations, computational investigations can study simple, ideal magnetic field configurations which cannot be produced in the laboratory. By first studying relatively simple, ideal magnetic fields, it is easier to understand the effects of different aspects of the magnetic field on the confinement length of complex magnetic field configurations that are produced by ring-cusp, permanent magnets.

For this analysis, three simple, ideal magnetic field configurations are studied: 1) a uniform magnetic field where the field lines run parallel to the sidewall of the discharge chamber as shown in Fig. 1, 2) a linearly increasing magnetic field where the field lines run parallel to the sidewall of the discharge chamber and increase from zero at a position 0.8 cm inside the wall to some finite value at the discharge chamber wall as shown in Fig. 2, and 3) a mostly uniform magnetic field where the field lines run parallel to the sidewall of the discharge chamber, except for openings that mimic cusp regions, as shown in Fig. 3. In these three simple, ideal magnetic field configurations, the magnetic field is concentrated close to the anode-biased side wall and penetrates into the discharge chamber a distance of 0.8 cm in the radial direction. In addition to showing the magnetic field lines, Figs. 1–3 show the path of one primary electron in the discharge chamber.

A simple, straight-cylindrically shaped, 10 cm long, 10-cm-diam discharge chamber with an 8 cm beam diameter is used for this analysis. A 2 A equivalent flow of xenon propellant is used along with a 30 V discharge potential. The simulation employs a 0.8 propellant utilization efficiency, a 0.4 grid transparency to ions, a 0.1 grid transparency to neutral atoms, and a neutral atom temperature of 348 K. A high propellant mass flow rate is considered so that the collision of primary electrons with other particles in the discharge chamber is enhanced. The front wall and the grids of the discharge chamber are forced to be cathode potential surfaces and therefore reflect electrons. The only anode-biased surface, (a surface that absorbs electrons) is the side of the cylindrical discharge chamber.

The nondimensional confinement lengths for the uniform field case and the linearly increasing ("sloped") magnetic field case including particle collisions are shown in Fig. 4. This figure shows that a 50 G uniform field strength keeps the primary electrons inside the discharge chamber for a fairly long time. A long time is defined as a confinement distance that allows approximately 90% of the primary electrons to undergo an ionizing collision. For the linearly sloped magnetic field, maximum field strengths of 10, 20, 50, 100, 150, and 200 G are analyzed. As Fig. 4 shows, primary electrons are able to penetrate the sloped magnetic field more easily than the uniform magnetic field. For the 0–50 G sloped field, the primary electron confinement length value is shortened by more than a factor of 7 from the value for the uniform 50 G field. It takes a 0–100 G sloped magnetic field to obtain similar confinement to that obtained with the uniform 50 G field.

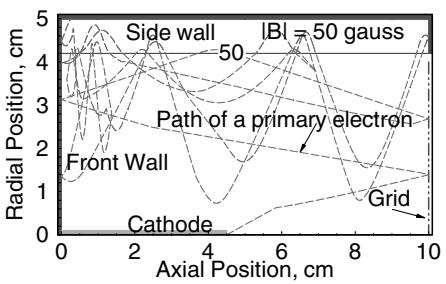

Fig. 1 Straight-cylindrical discharge chamber with a 0.8 cm thick, 50 G, uniform magnetic field covering the sidewall. One primary electron trajectory is also shown on the plot.

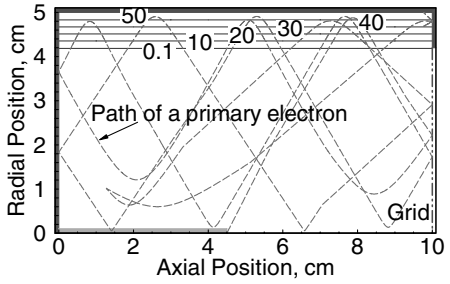

Fig. 2 Straight-cylindrical discharge chamber with a 0.8 cm thick linear varying magnetic field (given in gauss) covering the sidewall. One primary electron trajectory is also shown on the plot.

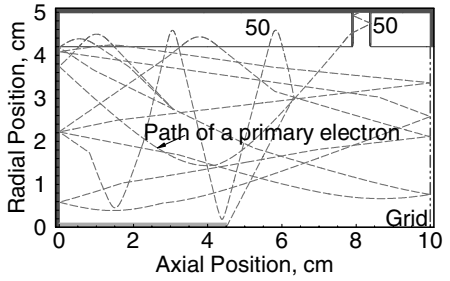

Fig. 3 Straight-cylindrical discharge chamber with a 0.8 cm thick, 50 G, uniform magnetic field covering the sidewall with holes. One primary electron trajectory is also shown on the plot.

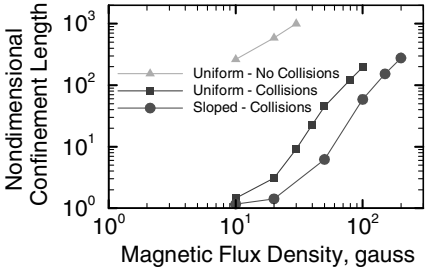

Fig. 4 Nondimensionalized confinement length as a function of the strength of a magnetic field for different simple, ideal magnetic field configurations and conditions.

Also shown in Fig. 4 are the effects of eliminating collisions from the analysis. The confinement lengths for a uniform magnetic field configuration with no particle collisions are much longer than those with particle collisions. Even a small uniform field strength of 10 G increases the primary electron confinement length to more than 200 times the value of a 10 G uniform field with particle collisions. Eliminating particle collisions from the computation also makes it computationally expensive to track every primary electron to absorption. For a 30 G field none of the particles were able to make it to the sidewall within a nondimensional time of 1000.

The third theoretical field configuration studied is a uniform magnetic field with holes as shown in Fig. 3. Holes in the field provide a path for primary electrons to reach the anode-biased walls. These holes can be viewed as the magnetic cusps formed in the ring-cusp magnetic field configuration or as weak fields between magnetic rings. Each hole is 0.5 cm wide and has a thin, strong radial field along the sides. The primary electron confinement length was analyzed for 1, 2, 3, and 4 holes in a 50 G uniform field configuration and the results are plotted in Fig. 5. Holes are added from the grid end

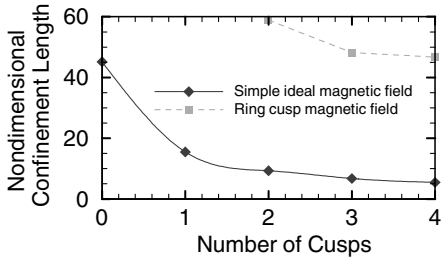

Fig. 5 Nondimensionalized confinement length for various numbers of holes (cusps) in a simple, ideal, uniform 50 G magnetic field covering the sidewall of a straight-cylindrical discharge chamber and for an actual ring-cusp magnetic field configuration.

of the discharge chamber back to the front wall. Putting one hole in the uniform magnetic field shortens the primary electron confinement length by 66% compared with the 50 G uniform magnetic field value with no holes. As the number of holes is increased, the value of the primary electron confinement length is reduced. The biggest reduction comes with the first hole, a much smaller reduction with the second hole, and an even smaller reduction with each succeeding hole. With four holes in the magnetic field the primary electron confinement length value is reduced by 88% from the value of the uniform 50 G field with no holes. This study shows that holes in the field shorten the confinement length. Quite naturally a very large number of holes would reduce the nondimensional confinement length to the no-field value of 1.1.

IV. Ring-Cusp Results

As opposed to the simple-ideal fields studied in the preceding section, actual, ring-cusp discharge chambers are studied in this section. The design parameter of the magnetic field studied is the number of magnetic rings. Other parameters that have been studied can be found in Mahalingam and Menart [1].

All of the ring-cusp discharge chambers results presented in this paper are for a conical-cylindrical shape discharge chamber with a chamber diameter of 10 cm and a chamber length of 10 cm. All the walls are made out of aluminum so they do not interact with the magnetic fields. The permanent magnets used to produce the magnet field are made out of samarium–cobalt and have a coercive force of −9300 oersteds and a residual magnetic field of 10,000 G. All chamber walls, except the grids, are taken to be at the anode potential. The grids are at a potential such that they attract ions and reflect all electrons that approach them. The tip of the cathode (location where the primary electrons are emitted) is located on the discharge chamber centerline 4.5 cm from the front wall. The other operating parameters used are the same as those used in the simple, ideal magnetic field study.

Results are presented for two, three, and four-ring discharge chambers. The confinement length results are shown in Fig. 5 along with the simple, ideal field results for a uniform magnetic field with holes. Results for the ring-cusp configurations follow the same trends as those for the ideal field configurations as a function of the number of cusps or holes. The longest confinement lengths are for the two-ring or two-hole configuration. Adding more rings or holes decreases the confinement length. The three-ring discharge chamber has a considerably shorter confinement length than the two-ring and a slightly longer confinement length than the four-ring configuration.

The obvious difference between the simple, ideal field results and the actual ring-cusp results is that the ring-cusp results are much larger than the simple, ideal field results. This indicates that cusps have better containment abilities than 0.5 cm wide holes. The reason for this is the mirroring [15] effect of the cusps.

Plots of the magnetic vector potential, the magnetic flux density, and the relative number density for the two-ring, ring-cusp discharge chamber can be found in Figs. 6–8. The same data for the three-ring discharge chamber and the four-ring discharge chamber can be found in Mahalingam [16]. The primary electron number density plot in Fig. 6 indicates that most electrons are being lost in the cusp regions

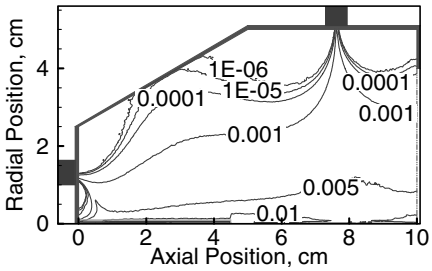

Fig. 6 Primary electron relative number density contours for a two-ring, conical-cylindrical discharge chamber.

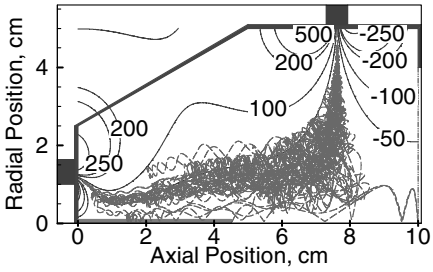

Fig. 7 Magnetic vector potentials in G-cm for a two-ring, conical-cylindrical discharge chamber. One primary electron trajectory is also shown on this plot.

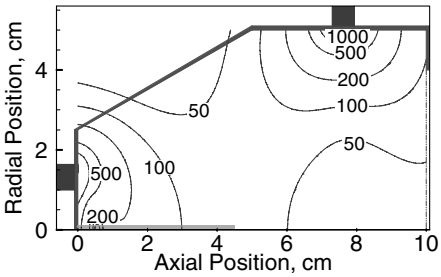

Fig. 8 Magnetic flux density contours in gauss for a two-ring, conical-cylindrical discharge chamber.

and that very few electrons are being lost to the walls between the magnet rings. Thus adding extra magnet rings provides more locations where primary electrons can be lost to the walls. The magnetic vector potential plot in Fig. 7 shows the direction of the magnetic field lines. Charged particles, like primary electrons, have difficulties crossing magnetic field lines, but travel freely along the field lines. The magnetic flux density plot shown in Fig. 8 shows the magnetic field strength distribution. The magnetic vector potential plots in combination with the magnetic flux density plots indicated that there are adequate magnetic fields present between the magnets to keep primary electrons from reaching the anode-biased walls. Lastly, one electron trajectory is shown in Fig. 7 to help the reader understand how a primary electron travels within the discharge chamber.

It must be realized that the results presented in this section are for a 10-cm-diam discharge chamber. For much larger diameter discharge chambers more rings may be needed to adequately cover the anode-biased walls between the magnets. Even though this is the case, the results presented in this paper indicate that the best primary electron confinement length is obtained with the fewest magnet rings required to adequately cover the walls.

V. Conclusions

A numerical code called PRIMA was used to analyze some simple, ideal magnetic field configurations and some actual ring-cusp magnetic field configurations. The purpose of this work was to ascertain which type of ring-cusp magnetic field best confines primary electrons in the discharge chamber. Only primary electron

confinement is considered and no attempt is made to deal with the issue of where ions are produced.

The simple, ideal field analysis presented in this paper indicates that a 50 G, uniform magnetic field that is 0.8 cm thick and parallel to the absorbing wall provides good primary electron containment. This simple, ideal field analysis also indicates that particle collisions greatly reduce the confinement ability of magnetic fields.

Actual, ring-cusp magnetic field configuration results show that cusp regions provide paths by which primary electrons can more easily reach an absorbing wall. This is shown by the simple, ideal field results as well. For this reason care should be taken in adding additional magnetic rings to a discharge chamber. Of course enough rings have to be used to provide adequate magnetic field coverage of all absorbing walls, but additional magnetic rings beyond this can actually reduce the confinement ability of the magnetic field. For a 10 cm conical-cylindrical discharge chamber that is 10 cm long, two rings of magnets provides better confinement than three and four magnet rings.

Acknowledgments

The authors would like to thank NASA John H. Glenn Research Center and Wright State University for financial support of this project.

References

[1] Mahalingam, S., and Menart, J., "Primary Electron Modeling in the Discharge Chamber of an Ion Engine," AIAA Paper 2002-4262, July 2002.

[2] Arakawa, Y., and Yamada, T., "Monte Carlo Simulations of Primary Electron Motions in Cusped Discharge Chambers," AIAA Paper 90-2654, July 1990.

[3] Isaacson, G. C., and Kaufman, H. R., "15-cm Multipole Gas Ion Thruster," *Journal of Spacecraft and Rockets*, Vol. 14, No. 8, Aug. 1977, pp. 469–473.

[4] Kaufman, H. R., Robinson, R. S., and Frisa, L. E., "Ion Flow Experiments in a Multipole Discharge Chamber," *AIAA Journal*, Vol. 22, No. 11, Nov. 1984, pp. 1544–1549.

[5] Ramsey, W. D., "12-cm Multi-Cusp Ion Thruster Inert Gas Performance," NASA CR-168208, 1984.

[6] Sovey, J. S., "Improved Ion Containment Using a Ring-Cusp Ion Thruster," *Journal of Spacecraft and Rockets*, Vol. 21, No. 5, 1984, pp. 488–495.

[7] Brophy, J. R., and Wilbur, P. J., "The Flexible Magnetic Field Thruster," *Journal of Spacecraft and Rockets*, Vol. 20, No. 6, 1983, pp. 611–618.

[8] Matossian, J. N., and Beattie, J. R., "Characteristics of Ring-Cusp Discharge Chambers," *Journal of Propulsion and Power*, Vol. 7, No. 6, 1991, pp. 968–974.

[9] Beattie, J. R., and Matossian, J. N., "Inert-Gas Ion Thruster Technology," NASA Lewis Research Center Contract Report, Contract NAS-3-23860, Sept. 1992.

[10] Sandonato, G. M., Barroso, J. J., and Montes, A., "Magnetic Confinement Studies for Performance Enhancement of a 5-cm Ion Thruster," *IEEE Transactions on Plasma Science*, Vol. 24, No. 6, Dec. 1996, pp. 1319–1329.

[11] Wirz, R., and Katz, I., "Plasma Processes of DC Ion Thruster Discharge Chambers," AIAA Paper 2005-3690, July 2005.

[12] Billen, J. H., and Young, L. M., "Poisson Superfish," Los Alamos National Laboratory document number LA-UR-96-1834, Revised 23 July 1998.

[13] Hiatt, J. M., and Wilbur, P. J., "Ring Cusp Discharge Chamber Performance Optimization," *Journal of Propulsion and Power*, Vol. 2, No. 5, Oct. 1986, pp. 390–397.

[14] Deshpande, S. S., Ogunjobi, T., and Menart, J., "Computational Study of Magnet Placement on the Discharge Chamber of an Ion Engine," AIAA Paper 2005-4254, July 2005.

[15] Chen, F. F., *Introduction To Plasma Physics*, Plenum Press, New York, 1974, Chap. 2.

[16] Mahalingam, S., "Primary Electron Modeling in the Discharge Chamber of an Ion Engine," M.S. Thesis, Mechanical and Materials Engineering Department, Wright State Univ., Dayton, OH, 2002.

A. Gallimore
Associate Editor